First Experimental Assessment of Protein Intrinsic Disorder Involvement in an RNA Virus Natural Adaptive Process

Justine Charon,*[,1,2] Amandine Barra,[1] Jocelyne Walter,[1] Pauline Millot,[3] Eugénie Hébrard,[4] Benoît Moury,*[,3] and Thierry Michon*[,1]

[1]UMR Biologie du Fruit et Pathologie, INRA, Université de Bordeaux, Villenave d'Ornon, France
[2]CNRS 5320, INSERM U1212, Pessac, France
[3]UR Pathologie Végétale, INRA, Montfavet, France
[4]UMR Interactions Plantes-Microorganismes-Environnement, IRD, CIRAD, Université de Montpellier, Montpellier, France

*Corresponding authors: E-mails: justine.charon@inra.fr; benoit.moury@inra.fr; thierry.michon@inra.fr.
Associate editor: Juliette de Meaux

Abstract

Intrinsic disorder (ID) in proteins is defined as a lack of stable structure in physiological conditions. Intrinsically disordered regions (IDRs) are highly abundant in some RNA virus proteomes. Low topological constraints exerted on IDRs are expected to buffer the effect of numerous deleterious mutations and could be related to the remarkable adaptive potential of RNA viruses to overcome resistance of their host. To experimentally test this hypothesis in a natural pathosystem, a set of four variants of *Potato virus Y* (PVY; *Potyvirus* genus) containing various ID degrees in the Viral genome-linked (VPg) protein, a key determinant of potyvirus adaptation, was designed. To estimate the ID contribution to the VPg-based PVY adaptation, the adaptive ability of the four PVY variants was monitored in the pepper host (*Capsicum annuum*) carrying a recessive resistance gene. Intriguingly, the two mutants with the highest ID content displayed a significantly higher ability to restore infection in the resistant host, whereas the less intrinsically disordered mutant was unable to restore infection. The role of ID on virus adaptation may be due either to a larger exploration of evolutionary pathways or the minimization of fitness penalty caused by resistance-breaking mutations. This pioneering study strongly suggests the positive impact of ID in an RNA virus adaptive capacity.

Key words: protein intrinsic disorder, potyvirus, RNA virus adaptation, resistance breakdown, viral protein genome-linked, eukaryotic translation initiation factor 4E.

Introduction

Protein intrinsic disorder (ID) defines proteins or protein regions that fail to fold into a unique 3D conformation under physiological conditions (Wright and Dyson 1999). A growing interest from the scientific community has been observed for this revolutionizing concept in the early 2000s. Large-scale investigations have led to recognize the ubiquity of ID among the whole living world, including viruses (Xue, Dunker, et al. 2012; Peng et al. 2014). Despite of their very limited overall size, some RNA virus proteomes possess the highest ID contents (Xue et al. 2012; Peng et al. 2014). The abundance of ID among RNA viruses could result from a strategy to cope with their very peculiar lifestyle and unique molecular characteristics (Alves and Cunha 2012; Xue et al. 2014). Indeed, one of the many noteworthy features of RNA viruses is their tiny genomes, currently comprised between 3,500 nt and 30,000 nt, which generally encode no more than a dozen of proteins (http://viralzone.expasy.org/; last accessed September 25, 2017; Hulo et al. 2011). Still, as obligatory parasites, RNA viruses need to recruit various host cellular components such as biological membranes, proteins and nucleic acids to accomplish their infectious cycles. Consequently, viral proteins are usually multi-functional and interact with multiple ligands. In this context, ID could be highly advantageous for RNA viruses by ensuring binding promiscuity. Indeed, many intrinsically disordered regions (IDRs) possess a high multiplicity of molecular interactions, partly illustrated by the high amount of ID in hub proteins (Haynes et al. 2006). Hence, the biophysical and dynamical properties of such regions are favorable to conformational rearrangements and molecular interaction switches, thus facilitating interactions with multiple partners. These extreme levels of structural plasticity could be also favorable to extend virus host range by enabling the recruitment of homologous factors expressed from different host species or genotypes in specific cases of recessive or nonhost resistances, or by enlarging the possibilities of molecular recognition disturbance in case of immune escape (Xue, Mizianty, et al. 2012). Beside binding promiscuity, a second advantage of ID in RNA viruses lies in the potential ability of such plastic regions to better accumulate and accommodate mutations. Indeed, IDRs generally display higher evolutionary rates compared with more-structured regions (Brown et al. 2002, 2010, 2011; Chen et al. 2006; Nilsson et al. 2011; van der Lee et al. 2014; Charon et al. 2016). Mechanistically, IDRs are characterized

Open Access

by lower contact densities between amino acid residues, which is expected to alleviate destabilizing effects of amino acid substitutions on viral protein stability and function (Tokuriki et al. 2009; Gitlin et al. 2014). RNA viruses display extraordinary high mutation rates, comprised between 10^{-3} and 10^{-5} errors/nucleotide/replication cycle (Duffy et al. 2008; Sanjuán et al. 2010), which contributes to place them as the fastest evolving entities on Earth and confers a great potential of fast adaptation to environmental disturbances (Drake 1999; Pfeiffer and Kirkegaard 2005). Consequently, the high mutation rates that result in sequence diversity and potentially adaptation of RNA viruses could be, at least partially, permitted by the ID of their proteins.

RNA viruses comprise the most damaging pathogens in both animals and plants. Their strong adaptive potential acts as a substantial barrier in the development of durable and efficient antiviral strategies in both medicine, veterinary and agricultural domains (Davenport et al. 2008; Pepin et al. 2010; Domingo et al. 2012). Understanding the genetic and molecular determinants of their capacity of adaptation still constitutes one of the major challenges in modern virology. The experimental assessment of the virus proteome ID contribution to host adaptation within a natural biological context is still in its beginning. We used the *Potato Virus Y* (PVY)/ *Capsicum annuum* (pepper) pathosystem to perform the first experimental analysis of the consequences of ID modifications on the adaptive potential of an RNA virus to its host. PVY, the type member of the large genus *Potyvirus* in the family *Potyviridae*, is one of the major viruses in plant pathology (Scholthof et al. 2011). In a preliminary study, by performing both inter and intraspecies analyses, we observed that, in potyviruses, ID regions display significantly higher dN/dS ratios (nonsynonymous and synonymous substitutions rates) than the ordered ones, which indicates the true tendency of IDRs to evolve faster than more structured regions during potyvirus evolution (Charon et al. 2016). Such weaker evolutionary constraints on IDRs strongly suggest the abilities for a faster and easier exploration of adaptive solutions. These results prompted us to further experimentally assess this hypothesis.

PVY infection in pepper involves numerous interactions between virus and host components. The multifunctional Viral genome linked protein (VPg) participates to several of them, and constitutes a major pathogenicity factor in potyviruses (Jiang and Laliberté 2011; Elena and Rodrigo 2012). The VPg has been experimentally characterized as intrinsically disordered in various potyviruses (Grzela et al. 2008; Rantalainen et al. 2008; Chroboczek et al. 2012). VPg IDRs are maintained within the whole *Potyvirus* genus, despite a high level of amino acid polymorphism, strongly suggesting a functional role of these regions in the virus fitness (Hébrard et al. 2009; Charon et al. 2016). Among these VPg IDRs, a central IDR is localized between residues 95 and 120, and harbors the determinants of PVY adaptation to the well-studied eukaryotic translation initiation factor 4E (eIF4E)-based recessive resistance (Moury et al. 2004; Ayme et al. 2006, 2007). A large majority of antiviral recessive resistances observed in plants involves eIF4E

(Wang and Krishnaswamy 2012). The eIF4E is an essential component of the translation initiation complex in eukaryotes and is hijacked by many RNA viruses for the translation and/or replication of their genomes. PVY adaptation to pepper eIF4E-mediated resistance can be viewed as a two-component molecular arm race, for which viral infection is directly linked to VPg-eIF4E molecular interaction (Charron et al. 2008). Thus, the colocalization of the central IDR and resistance-breaking sites in PVY VPg could typically illustrate the ID requirement for viral cycle and/or adaptation process. The novelty of our approach consisted in artificially modulating the ID content of this VPg central domain and analyzing the functional consequences of such alterations on PVY pathogenicity and adaptation to pepper eIF4E-mediated resistance.

Results

Obtention of Three PVY VPg Mutants ID1, ID2, and OD2 Affected in Their ID Content

Design of Mutation Combinations Predicted as Modulating the ID Level in the Central Region of VPg

Evaluating the impact of ID content on PVY adaptive potential first necessitates that the introduced mutations are not deleterious for VPg basal functionality. To maximize the probability of identifying such mutations, ID predictions were run on a data set of 35 VPg sequences of PVY isolates infecting pepper, collected worldwide (table 1; supplementary table S2, Supplementary Material online). Amino acid substitutions which, in the natural variability, led to the largest ID variations within the VPg central region, were introduced alone or in combination into PVY SON41p wild-type (WT) isolate (hereinafter named SON41p^WT; table 1; supplementary table S2, Supplementary Material online). Very importantly, this work aims to investigate the involvement of the VPg central ID as a favorable flexible environment that could enable the appearance of resistance-breaking mutations, and ultimately PVY adaptation. Thus, positions 101, 105, 115, 119, 121, and 123 which hold the single-residue resistance-breaking sites already linked to PVY adaptation to $pvr2^3$ (supplementary table S2, Supplementary Material online; Moury et al. 2004; Ayme et al. 2006, 2007) were voluntarily avoided to prevent any bias in the subsequent viral adaptation experiments (table 1). Three VPg mutants, named ID1 ($R_{94}G$; $D_{95}N$; $F_{100}L$), ID2 ($R_{94}G$; $D_{95}E$), and OD2 ($E_{102}Q$; $E_{114}Q$), were thus designed. Corresponding in silico predicted ID changes are reported in figure 1. For ID1 and ID2 mutants, 12% more residues were predicted as intrinsically disordered than in the WT VPg, with a higher probability of ID in ID1 than in ID2. For the OD2 mutant, PONDR-VLXT predicted 17% less disordered residues than in the WT VPg.

Assessment of ID Content in the Mutated VPgs by Circular Dichroism (CD) Spectroscopy

The impact of the introduced mutations on VPg structural properties was experimentally assessed. The CD spectrum of IDRs has a specific signature characterized by a minimum

Table 1. Identification of PONDR-VLXT Predicted VPg-SON41p Disorder-Affecting Amino Acid Substitutions Based on the VPg PVY (group C) Natural Genetic Diversity.

			93 I	94 R	95 D	96 I	98 E	100 F	101 S	102 E	105 R	108 V	114 E	115 T	117 A	118 L	119 D	121 H	123 S
VPg group C polymorphic sites	93	V	–																
	94	G			d														
	95	E, N				d													
	96	V				–													
	98	D					–												
	100	L						d											
	101	G							RB										
	102	Q								o									
	105	K									RB*								
	108	I										–							
	114	Q											o						
	115	A, M, R, T												RB					
	117	V													–				
	118	V														–			
	119	S, E, H															RB		
	121	N																RB*	
	123	K, E, N, T																	RB*

Second and third line/column: polymorphic amino acid sites and their corresponding positions in VPg protein sequence. Red/blue boxes: amino acids substitutions that are predicted (PONDR-VLXT) to enhance or reduce intrinsic disorder content in VPg-SON41p respectively. "d" and "o": respectively intrinsic disorder and order promoting substitutions; "RB": $pvr2^3$-resistance breaking sites previously identified (Ayme et al. 2006; Montarry et al. 2011); "RB*": expected resistance-breaking sites (displaying high dN/dS ratios; Ayme et al. 2007; Moury et al. 2014).
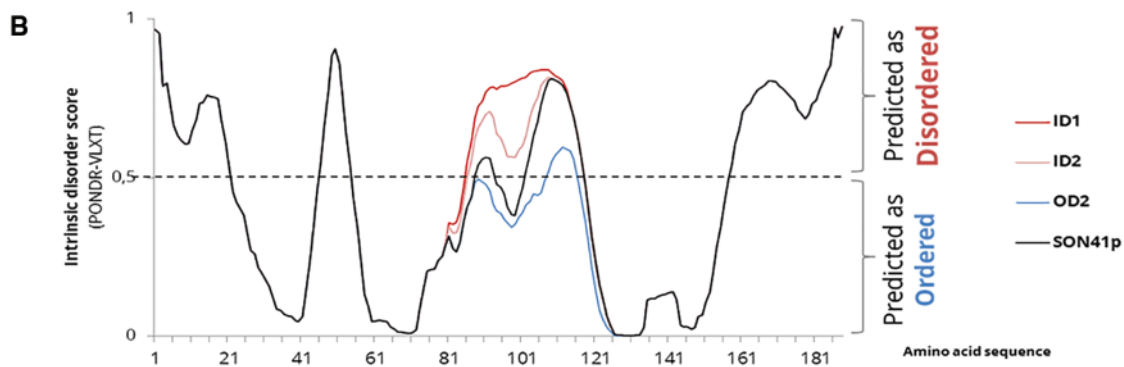

Fig. 1. The ID1, ID2, and OD2 VPg mutants. (*A*) Amino acid sequence of the central region of the VPg of PVY isolate SON41p[WT] and of its derived mutants ID1, ID2, and OD2. (*B*) Intrinsic disorder prediction (PONDR-VLXT) of the SON41p, and of VPg mutants ID1, ID2, and OD2. Residues with a score < or > 0.5 are considered as ordered or intrinsically disordered, respectively.

signal observed around 205 nm associated to a shoulder at 220 nm (Uversky 2002). Thus, one well-established strategy to compare ID content of proteins consists in determining their respective CD signal$_{205\,nm}$/CD signal$_{220\,nm}$ ratio, considering that higher ratios correspond to higher global ID contents (Woody 2010). The nucleotide sequences encoding WT, ID1, ID2, and OD2 VPgs were cloned in an *Escherichia coli* heterologous expression system from which the corresponding

proteins were produced. For each protein, CD spectra were obtained from 195 to 250 nm (fig. 2A). 205/220 nm ratios confirmed that OD2 was significantly less intrinsically disordered than the WT VPg. Conversely, ID1 and to a lesser extent ID2 were significantly more intrinsically disordered than WT VPg (fig. 2B). Interestingly, these data were in very good agreement with in silico predictions. This particular case illustrates the potential robustness of PONDR-VLXT to predict ID
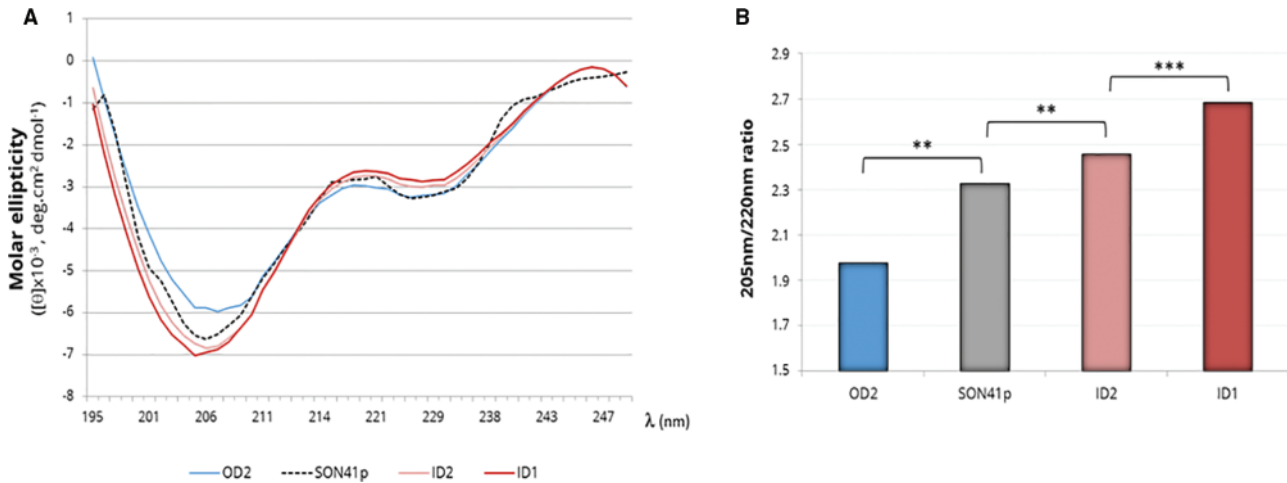
Fig. 2. Circular dichroism signal of the VPg of PVY SON41p and of mutants ID1, ID2, and OD2. (A) Molar ellipticities obtained for λ comprised between 195 and 250 nm. (B) 205 nm/220 nm molar ellipticity ratios calculated for each VPg. "**" and "***" correspond to P-values ≤ 0.01 and 0.001, respectively (Kruskal–Wallis test).

content. It is worth mentioning that the CD signal results from the contribution of the whole VPg secondary structure. However, although it is not possible to formally exclude that the introduced changes in the VPg central region could have long-range effects on the VPg structure, it is more likely that the observed variations in ID levels are located in the VPg central region.

Effects of ID-Affecting Mutations on PVY Infectivity and Accumulation in Yolo Wonder Susceptible Pepper

As previously indicated, analyzing the impact of mutations affecting ID on the adaptive capacity of PVY on resistant hosts first requires to ensure that such mutations do not affect the virus cycle in a susceptible host context. To this end, SON41p[WT] mutants carrying either ID1, ID2, or OD2 VPg coding sequences (named SON41p[ID1], SON41p[ID2], and SON41p[OD2], respectively) were inoculated in Yolo Wonder pepper plants carrying the pvr2[+] susceptibility allele. The numbers of symptomatic plants and the corresponding viral accumulation from two independent assays were determined 30 days postinoculation (dpi) and are presented in figure 3.

As for SON41p[WT], 100% of plants inoculated with SON41p[ID1], SON41p[ID2], and SON41p[OD2] displayed mosaic symptoms in apical noninoculated leaves as soon as 10 dpi for both the 2015 and 2016 assays (fig. 3A). Crucially, DAS-ELISA (double antibody sandwich-enzyme-linked immunosorbent assay) revealed a similar viral accumulation for the four PVY variants in Yolo Wonder plants at 30 dpi (fig. 3B).

To control for the stability of SON41p[ID1], SON41p[ID2], and SON41p[OD2] during infection and to confirm that the virus phenotype was not linked to further evolution within the plants, ten plants per mutant were subjected to total RNA extraction and Sanger sequencing of the PVY VPg cistron. In addition, three plants per mutant were randomly chosen for PVY full-genome sequencing. When compared with the initial sequence, no additional mutation or mutation reversion

was detected. These results confirmed that the mutations introduced to create the SON41p[ID1], SON41p[ID2], and SON41p[OD2] mutants are not deleterious for PVY infectivity. More precisely, they do not affect the ability of the virus to infect Yolo Wonder, as attested both by the viral accumulation and symptoms and considering that the consensus sequence of the PVY populations remained unchanged during the infection process.

Effect of ID-Affecting Mutations on PVY Ability to Adapt to the pvr2[3]-Mediated Resistance

As previously introduced, adaptation of PVY SON41p to eIF4E-mediated pvr2[3] resistance is convenient to study the determinants of RNA virus adaptation as it is well-characterized and because of the experimental advantages it provides. Indeed, pvr2[3]-resistance breaking by SON41p is fast (necrotic symptoms appear between 20 and 30 dpi) and partial, as around 20–40% of pvr2[3] plants become infected after the appearance and fixation of VPg mutations in the PVY population (Ayme et al. 2006; Montarry et al. 2011). Consequently, it is easily attainable to estimate if an external (environment, plant genetic background) or internal (virus genetic alterations) factor increases or decreases SON41p adaptation capacity. Moreover, it was previously demonstrated that pepper pvr2[3]-mediated resistance and the corresponding PVY adaptation is a two-component system, in which infection is determined mostly by the physical interaction between plant eIF4E and the viral VPg (Charron et al. 2008; Moury et al. 2014). The HD285 pepper line, carrying the pvr2[3] resistance gene, essentially differs from Yolo Wonder at the pvr2 locus (see Materials and Methods) and allows us to consider that the differences in PVY infectivity observed between Yolo Wonder and HD285 are essentially due to differences in binding affinity between PVY VPg and plant pvr2-encoded eIF4Es.

To assess the consequence of altering the ID of the VPg central domain on the PVY ability to adapt to the pvr2[3] resistance, SON41p[WT], SON41p[ID1], SON41p[ID2], and
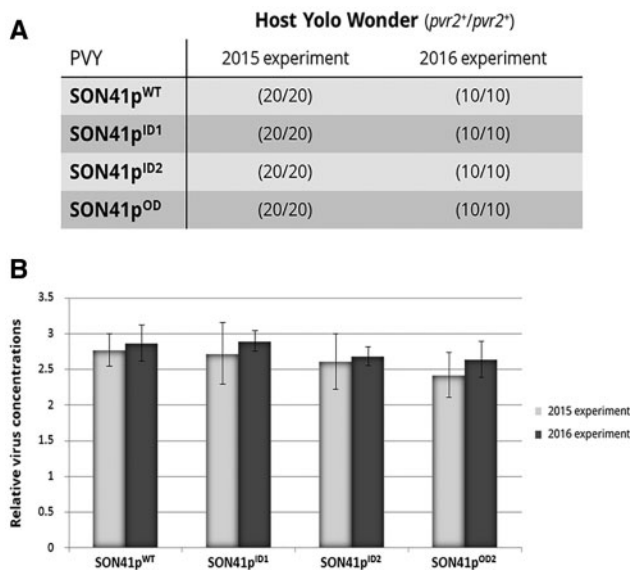
A

Host Yolo Wonder $(pvr2^+/pvr2^+)$		
PVY	2015 experiment	2016 experiment
SON41p[WT]	(20/20)	(10/10)
SON41p[ID1]	(20/20)	(10/10)
SON41p[ID2]	(20/20)	(10/10)
SON41p[OD]	(20/20)	(10/10)

B

Fig. 3. Infectivity properties of SON41p[WT] and the PVY mutants SON41p[ID1], SON41p[ID2], and SON41p[OD2] on Yolo Wonder host. (A) Number of symptomatic plants observed after inoculation of SON41p[WT] and the PVY mutants SON41p[ID1], SON41p[ID2], and SON41p[OD2] on Yolo Wonder host for the two independent experiments conducted in 2015 and 2016. Values indicate numbers of infected plants (symptoms and/or virus accumulation) among inoculated plants; (B) DAS-ELISA determination of PVY relative accumulation on Yolo Wonder pepper host at 36 days post inoculation. White and grey bars represent data obtained in the 2015 and 2016 experiments, respectively. Within each experiment, no significant differences were observed between the four PVY variants (Mann–Whitney U tests; P-values > 0.05). Standard deviations are indicated on each bar.

SON41p[OD2] were inoculated to 120 HD285 plants. The capacity of WT PVY and PVY mutants to breakdown the $pvr2^3$ resistance (i.e., to accumulate and induce symptoms on HD285) were compared at 36 dpi. Results of the two independent 2015 and 2016 experiments are presented in figure 4. Infection by SON41p was observed in 22% (2015) to 39% (2016) of $pvr2^3$-inoculated plants, in good agreement with previously published data (Ayme et al. 2006). Very interestingly, the SON41p[OD2] mutant, carrying an ID-depleted VPg, was unable to overcome the $pvr2^3$ resistance, as no symptomatic and/or DAS-ELISA positive plants were observed among the 120 and 50 inoculated. SON41p[ID2] mutant displayed a significantly higher capacity of infection compared with PVY SON41p[WT], with between 1.6 and 2.3 times more infected plants. Finally, SON41p[ID1] mutant reached the highest infectivity, as 2.3–3 times more of inoculated plants were infected (fig. 4A) compared with SON41p[WT].

Analysis of Molecular Events Underlying Infection of PVY SON41p[WT], SON41p[ID1], SON41p[ID2], and SON41p[OD2] in $pvr2^3$-Carrying Pepper Plants
Analysis of VPg Sequence Modifications in $pvr2^3$-Carrying Plants

In a view to understand the large differences of infectivity in HD285 observed between PVY SON41p[WT] and the two
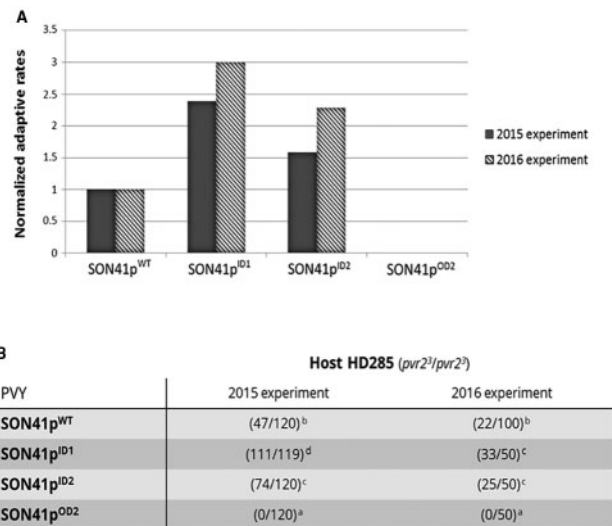
A

B

Host HD285 $(pvr2^3/pvr2^3)$		
PVY	2015 experiment	2016 experiment
SON41p[WT]	(47/120)[b]	(22/100)[b]
SON41p[ID1]	(111/119)[d]	(33/50)[c]
SON41p[ID2]	(74/120)[c]	(25/50)[c]
SON41p[OD2]	(0/120)[a]	(0/50)[a]

Fig. 4. Infectivity properties of SON41p[WT] and the PVY mutants SON41p[ID1], SON41p[ID2], and SON41p[OD2] on HD285 pepper hosts. (A) Normalized adaptive rates observed after inoculation of the PVY mutants SON41p[ID1], SON41p[ID2], and SON41p[OD2] on HD285 host compared with SON41p[WT]. (B) Total numbers of infected HD285 plants after inoculation of the SON41p[WT] and PVY mutants SON41p[ID1], SON41p[ID2], and SON41p[OD2] for the two independent 2015 and 2016 experiments. Values in brackets indicate numbers of infected plants (symptoms and/or virus accumulation) among inoculated plants and the corresponding percentages. a–d: groups with statistically significant differences independently obtained within 2015 (left) and 2016 (right) experiments (Fisher exact tests using 2×2 contingency tables and Bonferroni correction for multiples testing; P-values < 0.001).

mutants SON41p[ID1] and SON41p[ID2], total RNAs were extracted from 10 to 20 randomly-chosen plants infected, for each of the three viruses. Sanger sequencing of the full virus genome and/or VPg-cistron were conducted (see Materials and Methods). No mutation was observed outside the VPg cistron. VPg sequencing results are provided in figure 5 and refer to sequences obtained in the 2015 and 2016 assays. The VPg of SON41p[ID1] mutant remained non-mutated in 94% (2015) and 90% (2016) of the sequenced samples (fig. 5A). By contrast, SON41p[WT] and SON41p[ID2] progenies displayed a minority of nonmutated VPg representing between 0% and 22% of the viral populations (fig. 5A). Unlike SON41p[ID1], infections of HD285 by SON41p[WT] and SON41p[ID2] mutant are largely associated to additional mutations in the VPg.

Regarding mutated VPgs in the progenies of SON41p[WT], four different amino acid substitutions were identified. The majority of these mutations were reported previously (fig. 5B; Ayme et al. 2006; Montarry et al. 2011) and two of them were shown to be responsible for adaptation of SON41p[WT] to $pvr2^3$ by reverse genetic experiments (mutations $D_{119}N$ and $T_{115}K$). Worth mentioning, $S_{120}T$ had never been described so far and may constitute a new $pvr2^3$-resistance-breaking mutation. Our sequencing results also confirmed the large proportion of $D_{119}N$ among SON41p[WT] resistance-breaking variants as previously reported (Ayme et al. 2006; Montarry et al. 2011).
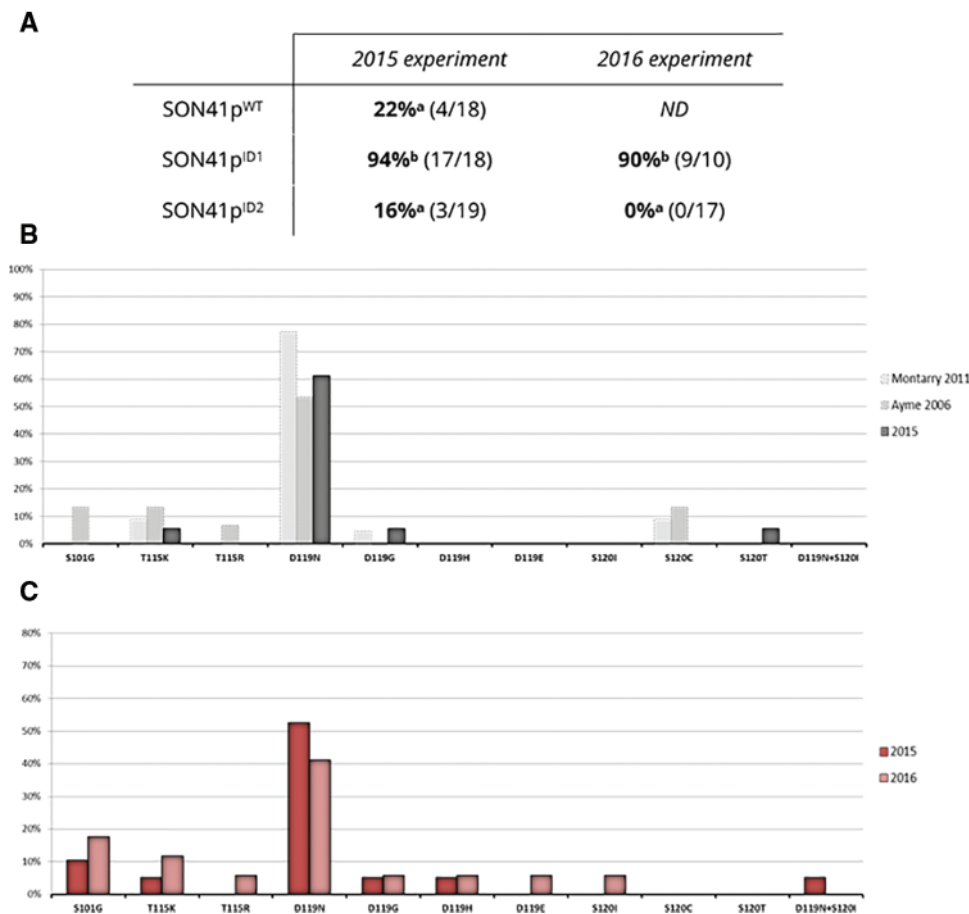
FIG. 5. Frequencies of VPg amino acid substitutions associated to infection of $pvr2^3$-carrying HD285 pepper plants by PVY SON41p[WT] and SON41p[ID2]. (A) Proportion of nonmutated VPg associated to infection of $pvr2^3$-carrying plants after inoculation with SON41p[WT], SON41p[ID1], or SON41p[ID2] PVY mutants, among the total number of sequenced PVY populations obtained from individual infected plants. "a" and "b": groups with statistically-significant differences independently obtained within 2015 and 2016 experiments using Fisher exact tests and Bonferroni correction for multiple testing (2×2 contingency tables; P-values < 0.001). ND: no virus population was sequenced. (B) Amino acid substitutions observed in virus populations derived from SON41p[WT] PVY in infected HD285 plants. Dotted bars refer to observations reported from (Ayme et al. 2006; Montarry et al. 2011). (C) Amino acid substitutions observed in virus populations derived from SON41p[ID2] PVY in infected HD285 plants.

As for SON41p[WT], a large proportion (40–50%) of SON41p[ID2] resistance-breaking variants carried the $D_{119}N$ substitution. Other mutations, observed in few samples, have already been validated for their role in adaptation to $pvr2^3$ by reverse genetics ($T_{115}K$, $T_{115}R$, and $S_{101}G$) or observed in previous experiments ($D_{119}G$). In addition, four mutations which have never been described so far in SON41p[WT] and were observed in PVY progenies, namely $D_{119}H$, $D_{119}E$, $S_{120}I$, and $D_{119}N + S_{120}I$. Although these results reveal a tendency of PVY mutant SON41p[ID2] to display more diversified adaptive solutions (eight different substitutions in total) than those identified for SON41p[WT] (four in total), a Shannon diversity comparison showed that this difference was not statistically significant (supplementary fig. S1, Supplementary Material online).

Analysis of the Thermodynamic Binding Strengths of the eIF4E/VPg Complex
Analysis of mutations in the VPg from $pvr2^3$-resistance break-ing variants was not sufficient to understand the strong differ-ences observed in infectivity between SON41p[ID1], SON41p[ID2],

SON41p[WT], and SON41p[OD2]. An attempt was made to relate these differences to the binding strength between the mu-tated VPgs and either the susceptible or resistant form of eIF4E, respectively carried by Yolo Wonder ($pvr2^+/pvr2^+$) and HD285 ($pvr2^3/pvr2^3$) peppers. Steady-state fluorescence spectroscopy was used to measure dissociation constants (K_d) between $pvr2^+$-eIF4E or $pvr2^3$-eIF4E and VPgs WT, ID1, ID2, and OD2, according to Michon et al. (2006). The K_d values of the VPg/eIF4E interactions were measured from two independent assays (see Materials and Methods) and are expressed relative to K_d obtained for the SON41p[WT] VPg/$pvr2^+$ eIF4E combination conducted in the same exper-iment (fig. 5). To ensure that the two eIF4E forms were stable and fully functional, their ability to interact with a eukaryotic 5′-cap analog m7-GTP was systematically assessed and pro-vided a K_d in the same range (around 300 nM) than those observed previously for lettuce eIF4E (Michon et al. 2006; *data not shown*), attesting the integrity of eIF4E samples used in these experiments.

The affinity of the WT VPg for $pvr2^3$-eIF4E was about two times lower than for $pvr2^+$-eIF4E (fig. 6). These results could
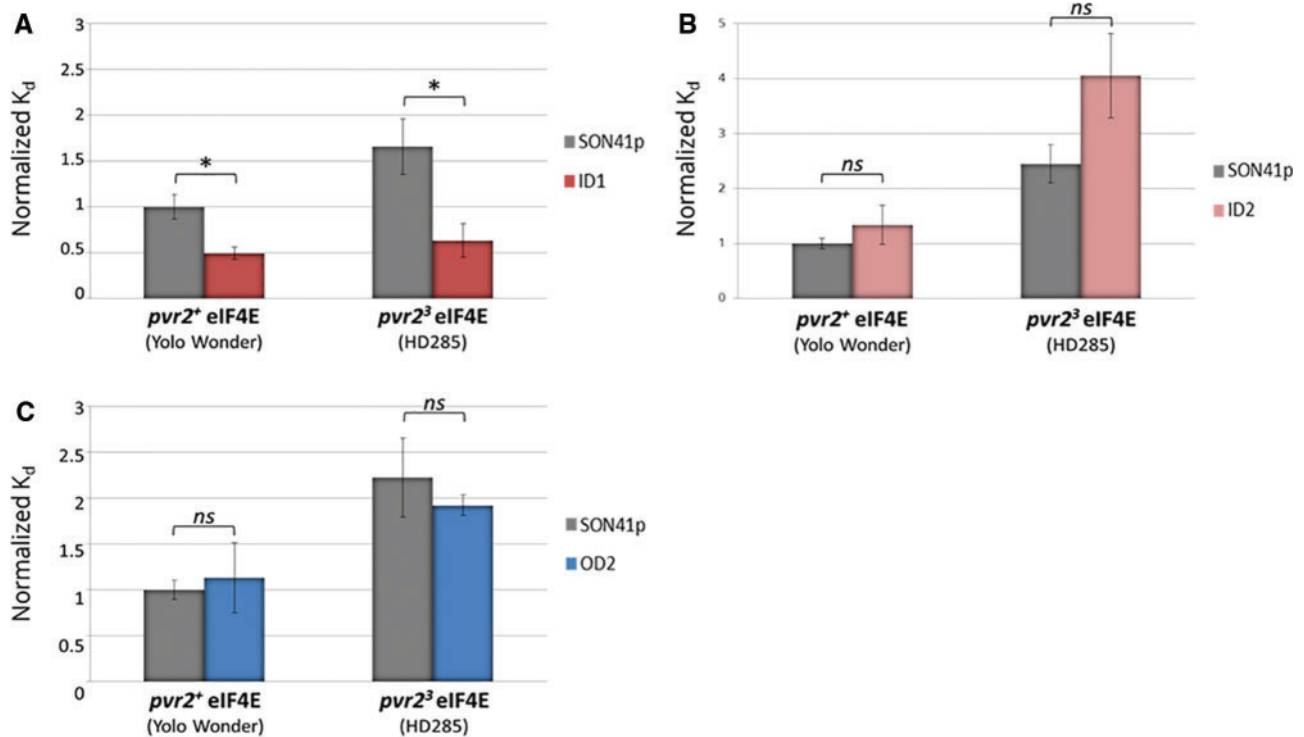
Fig. 6. Relative in vitro dissociation constant (K_d) between *pvr2*-encoded pepper host eIF4E and wild-type (SON41p) or mutated (ID1, ID2, and OD2) PVY VPgs. *Left*: interaction with *pvr2*+-encoded eIF4E. *Right*: interaction with *pvr2*³-encoded eIF4E. (A) Normalized K_d obtained after comparing interaction with SON41p (grey) and ID1 (red). (B) Normalized K_d obtained after comparing interaction with SON41p (grey) and ID2 (pink) VPgs. (C) Normalized K_d obtained after comparing interaction with SON41p (grey) and OD2 (blue) VPgs. "*" and "*ns*": statistically significant and nonsignificant differences, respectively (based on 95% confidence intervals). Standard deviations obtained from the method used to determine each K_d (see Materials and Methods) are shown on each bar. *Note that K_d is inversely related with binding affinity.*

explain the requirement of additional mutations in the VPg for PVY adaptation to *pvr2*³ resistance and demonstrate, once again, the tight link between VPg/eIF4E interaction and PVY infection in pepper. More precisely, the pepper *pvr2*³ resistance to PVY could be due to a low affinity between eIF4E and VPg, preventing PVY to establish infection in *pvr2*³ peppers rather than a total inability to interact with *pvr2*³-encoded eIF4E. Additionally, it could also explain why PVY SON41pᵂᵀ is able to evolve in the *pvr2*³-carrying plants and reach adaptive solutions during the 36 days following inoculation. Conversely, the highly intrinsically-disordered ID1 VPg interacted with *pvr2*³-eIF4E with an affinity 3 times higher than SON41pᵂᵀ VPg, while maintaining its ability to recruit the *pvr2*+-eIF4E form (fig. 6A). ID2 and WT VPgs displayed the same affinity with the *pvr2*+-eIF4E form but ID2 interacted with *pvr2*³-eIF4E with a lower affinity than that observed for WT VPg (fig. 6B).

Concerning the more structurally-ordered OD2 VPg, we noticed that affinities of its in vitro interactions with each *pvr2*+ and *pvr2*³ eIF4Es were similar to those of the WT VPg (fig. 6C).

Discussion

Assumptions regarding the involvement of protein ID in viral adaptive capacity and adaptation process still rely on in silico predictions and functional hypotheses. To date, no experimental data has been reported in the literature to challenge

these assumptions. This work intends to test experimentally the contribution of the ID of a viral protein in the virus host adaptation. The PVY-pepper couple is remarkably convenient for this, as the effect of disorder modulations within the viral VPg on virus infectivity can be followed on a large set of host plants under true biological conditions. We generated three PVY mutants with a modified amount of ID in the VPg pathogenicity factor. Remarkably, and for the first time, it was observed that ID modifications were linked to strong differences in virus infectivity and adaptive behavior.

Causal Link between ID Modifications and Alteration in Virus Phenotypes

ID is strictly sequence-dependent. Accordingly, every attempt to modify the ID within a protein inevitably entails a change in its amino acid sequence. In our approach to artificially modify ID within the VPg, a multifunctional protein involved in various steps of PVY cycle, it cannot a priori be excluded that some phenotypic observations result more from the very nature of amino acid substitutions than from the ID changes they induced. The fact that no effect of the introduced mutations was observed on PVY pathogenicity in the susceptible host Yolo Wonder strongly suggests that there is no bias of this kind. The choice of the mutations to be introduced was intended to uncouple the ID itself from previously identified resistance-breaking codon positions. In the case of ID1 and ID2, all mutations were chosen outside of the VPg region

involved in resistance breakdown which spans from amino acid position 101 to 123 (Ayme et al. 2006; Montarry et al. 2011). Conversely, the two mutations conferring an order increase to OD2 were located within the resistance breaking region (table 1). In that case, we postulated that substitutions at positions that have never been observed as associated to resistance-breaking events were unlikely to induce resistance-breaking by their own. In fact, the opposite effect was observed, since SON41p[OD2] was completely unable to infect the HD285 pepper genotype carrying the pvr2[3] resistance. Thus, even if a direct causal link between ID changes and virus phenotypes alterations cannot be formally established, our experimental strategy leads us to postulate that the mutant phenotypes observed in this study are more than likely induced by the underlying ID changes.

Is ID an Expander of VPg Binding Spectrum Leading to an Enlargement of PVY Host Range?

The three amino acid substitutions in ID1 VPg central region have significantly increased the ID of the VPg and are associated to a sharp improvement of SON41p[ID1] infectivity toward pvr2[3]-carrying pepper plants compared with SON41p[WT]. The lack of additional mutations in the VPg (or elsewhere in the genome) of most of the SON41p[ID1] progenies indicates that the increased ability of SON41p[ID1] PVY to infect these plants does not rely on adaptive mutations that would occur after inoculation in resistant host but more likely on the intrinsic capacity of SON41p[ID1] to infect the pvr2[3] plants. Considering the direct link that exists between VPg/eIF4E binding and infection in the PVY/pepper pathosystem (Charron et al. 2008), the significant increase of the ID1 VPg affinity for both pvr2[+]-eIF4E and pvr2[3]-eIF4E compared with WT VPg could largely be responsible for the higher SON41p[ID1] infectivity. In addition, it could explain that the host range expansion was not traded-off against a decrease of infectivity in Yolo Wonder host. Through its inherent structural flexibility, the VPg central IDR could expand its interaction spectrum to eIF4E forms of closely-related pepper cultivars according to mechanistic principles of ID functionality in hub proteins (Haynes et al. 2006). Ultimately, this would lead to an enlargement of the virus infection spectrum.

Is ID a Fuel for PVY Resistance Breakdown in pvr2[3]-Carrying Plants?

As ID1, VPg mutant ID2 is characterized by an increase of ID level in its central IDR, associated to a significant increase of resistance-breaking events in pvr2[3] host compared with SON41p[WT]. However, molecular mechanisms underlying those observations seem radically distinct from those explaining the phenotype of SON41p[ID1]. In the case of SON41p[ID2] in pvr2[3] plants, infection cases are near-exclusively associated to the appearance of additional mutations in the VPg, similar to those previously reported as responsible for the breakdown of the pvr2[3] resistance by SON41p[WT] (Ayme et al. 2006; Montarry et al. 2011). In addition, the ID2 VPg affinity for pvr2[+]- and pvr2[3]-eIF4Es are respectively similar and lower than those measured for WT-VPg. These binding strength discrepancies cannot account for the significant differences

of resistance-breaking rates observed between SON41p[WT] and SON41p[ID2]. Considering the general potential of IDRs to evolve faster and to better accommodate mutations, a hypothesis to explain the higher adaptive capacities of SON41p[ID2] compared with SON41p[WT] in the pvr2[3]-carrying host could be that the higher ID in the VPg of SON41p[ID2] is associated to a larger mutational robustness of the VPg central region. Such an effect would allow 1) an enhanced tolerance to the resistance-breaking mutations already associated to SON41p[WT] adaptation; 2) the emergence of additional adaptive solutions. In both these nonexclusive mechanisms, ID increase would lead to a higher adaptive potential. Despite its basal ability to replicate in pvr2[3]-carrying host HD285, PVY needs to evolve and accumulate mutations in its VPg in view of maintaining itself and restoring infection in the plant. Consequently, adaptation of the virus lies in its ability to accumulate mutations in the VPg and gain sufficient fitness for efficiently colonizing the host plant while countering its basal defenses. Whereas the kinetics of mutation appearance relies exclusively on the viral replicase mutational rate, the relative fitness of each variant can result from structural properties of their pathogenicity factor—that is, the VPg in the case of PVY adaptation to pvr2[3]. Thus, the higher mutational robustness in IDRs could lead resistance-breaking variants to accumulate faster in the host, leading to a higher probability of restoring systemic infection and ultimately of adapting. As a matter of fact, although statistically nonsignificant, it can be observed that, for a similar number of variants sequenced in each study (comprised between 15 and 22), SON41p[ID2] displays a tendency to accumulate more diverse resistance-breaking variants than SON41p[WT].

Finally, the analysis of the SON41p[OD2] PVY mutant remarkably reinforces our hypothesis. Indeed, the decrease of ID generated by the $E_{102}Q$ and $E_{114}Q$ substitutions introduced into OD2 VPg did neither affect PVY infectivity in Yolo Wonder nor the VPg affinity for pvr2[+] or pvr2[3]-encoded eIF4Es, compared with SON41p[WT] and WT VPg, respectively. Consequently, the inability of SON41p[OD2] to adapt to the pvr2[3] resistance results most likely from a disability of this mutant to accumulate adaptive mutations during its evolution in the resistant host, rather than from a deleterious effect of the $E_{102}Q$ and $E_{114}Q$ mutations on its intrinsic infection capacity. By reducing the VPg ID, the mutations introduced in OD2 could reduce SON41p[OD2] tolerance to amino acid substitutions, thereby reducing the probability of adaptive events to occur.

Is ID in VPg Central Region Dispensable for PVY Infectious Cycle?

It was observed in this study that the decrease of ID in the central region of the VPg mutant OD2 does not seem to affect PVY infectivity in the Yolo Wonder pepper plants carrying the susceptibility allele pvr2[+]. One of the functional aspects of IDRs is their ability to ensure interactions with multiple molecular partners (Haynes et al. 2006; Cumberworth et al. 2013). The well-established multifunctional and multi-interacting nature of the VPg protein (Jiang and Laliberté 2011; Elena and Rodrigo 2012; Martínez et al. 2016) and more specifically of its central domain

(Roudet-Tavert et al. 2007) appears as not ultimately dependent on a highly defined ID, despite the evolutionary conservation of this structural feature among potyviruses (Charon et al. 2016). Nevertheless, functional involvement of ID in VPg multiple interactions still remains to be elucidated, as ID is also predominant and conserved in others VPg regions (N-ter and C-ter) and could be responsible for VPg multiple interaction capacities.

Establishing ID Content of Viral Proteins as an Additional Criterion in the Design of Antiviral Strategies

This study reports a body of information strongly arguing for an impact of ID level of viral proteins on the virus adaptation to host resistance. In order to assess the extent of ID-driven adaptation in virus biology, similar experiments should be performed for other viral proteins and other cases of virus adaptation. Beyond their advantages compared with animal viruses in terms of biosafety, phytoviruses are particularly suited for evolutionary experiments as the biological properties of mutants can be quickly and accurately tested against a rich collection of host plants and the evolution of viral progenies can be easily analyzed in vivo without the ethical restrictions linked to inoculation of animals with genetically-modified viruses. In potyviruses, VPg does not constitute the only pathogenicity factor displaying resistance-breaking determinants associated to evolutionary-conserved IDRs. Lettuce mosaic virus (LMV) resistance-breaking sites have been located in a highly-conserved IDR (Charon et al. 2016) of the virus helicase (Abdul-Razzak et al. 2009). Investigating more distant pathosystems appears as essential and could also include sobemoviruses for which adaptive mutations are also located within IDRs (Hébrard et al. 2009). Demonstrating the ubiquitous nature of ID as a determinant of RNA virus adaptation would be of major importance for the whole virologist community and is expected to greatly enhance our global understanding of RNA virus adaptation processes and our ability to anticipate those events. At the molecular levels, host resistance durability against viruses results both from the number of mutations necessary for the virus to adapt and the fitness penalty associated to each of them (Harrison 2002; Jenner et al. 2002; Ayme et al. 2007). Resistance durability has been correlated to evolutionary constraints exerted on pathogenicity factors involved in viral adaptation (Janzac et al. 2009). Measuring evolutionary rates of pathogenicity factors appears to be an efficient measure to predict the durability of plant resistance and more generally of antiviral control methods. Ultimately, establishing a more general link between ID and RNA virus adaptation could promote this easily predictable structural feature as a new criterion to include in the design of antiviral control methods. Indeed, owing to their adaptive abilities, viral IDRs could constitute poor targets of both drugs and host genetic resistance that constitute the main antiviral strategies in animal and plants.

Materials and Methods

Plant and Virus Materials

PVY isolate SON41p (accession number AJ439544) was used as the reference WT genotype. All PVY mutants were derived from this genotype. Natural hosts *Nicotiana benthamiana* and *C. annuum* accessions Yolo Wonder and HD285 carrying respectively $pvr2^+/pvr2^+$ and $pvr2^3/pvr2^3$ genotypes were used for experiments. HD285 is a doubled-haploid line derived from the F_1 hybrid (Yolo Wonder × Perennial) and genetically selected for PVY SON41p resistance allele $pvr2^3$ and susceptibility alleles at the other loci (Caranta et al. 1997). The 35 PVY isolate sequences used for designing VPg mutations belong to PVY group C1 that infects *C. annuum* are listed in supplementary data (supplementary table S1, Supplementary Material online).

Computational and Experimental ID Characterization

In silico preliminary predictions of VPg ID content were performed using Predictor of Naturally Disordered Regions (PONDR-VLXT), accessible through the Disprot server (http://disorder.compbio.iupui.edu/metapredictor.php; last accessed September 25, 2017; Sickmeier et al. 2007; Xue et al. 2010). Parameters were set to "default" for ID score predictions.

In vitro experimental characterization of ID was assessed using far UV CD measurements on the different recombinant VPg forms. Molar ellipticities were recorded at 20 °C under nitrogen using a Jasco-815 spectropolarimeter. Samples consisted in 0.1 mg/ml pure VPg forms in 0.02 M sodium phosphate, 0.3 M sodium fluoride, pH 8. In these conditions, using 1 mm optical path cuvette, the photomultiplier tube dynode voltage did not exceed 380 V at 190 nm, which permitted a satisfactory spectral resolution from 200 nm and above.

PVY Inoculation and Detection

Infectious mutated PVY clones were obtained after NotI-linearization of a plasmid containing the sequence of SON41p[WT] except the central part of the VPg-coding sequence followed by homologous recombination in yeast (*Saccharomyces cerevisiae* strain YPH501) with PCR products corresponding to ID1, ID2 or OD2 VPg-coding sequences, as previously described in Ayme et al. (2006). Infectious clones were recovered from yeast and cloned into *E. coli*, strain Max-efficiency DH10B (New England Biolab, NEB), to ensure sufficient amounts of plasmids. The direct biolistic inoculation of full length PVY cDNA clones does not produce infection in *C. annuum* (Moury et al. 2004), and a preliminary inoculation in three-week old *N. benthamiana* plants was required. Inoculated plants were grown under controlled conditions and symptomatic leaves were retrieved at 15 dpi (supplementary fig. S2, Supplementary Material online). To ensure that the virus population did not evolve in the *N. benthamiana* plants used to prepare inocula, full-genome Sanger sequencing was performed on total RNA isolated from each leaf extracts used to inoculate pepper plants. In each case, the initial PVY sequences were found, precluding any major virus evolution within *N. benthamiana*. Viral loads were

determined using quantitative DAS-ELISA semiquantitative assays (Ayme et al. 2006) using home-made polyclonal antiPVY antibodies. When necessary, the volume of leaf extracts was adjusted with phosphate inoculation buffer to ensure the same virus concentration between virus inocula. The resulting calibrated inocula were used to mechanically inoculate cotyledons of three-weeks-old Yolo Wonder and HD285 peppers, as described in Moury et al. (2004). The effects of virus inoculation on Yolo Wonder were assessed after 30 days, and, in the case of HD285, between 36 and 45 days after inoculation. A successful infection was associated with mosaic and necrotic symptoms on upper non-inoculated leaves for HD285 and mosaic only for Yolo Wonder (supplementary fig. S2, Supplementary Material online). The viral load in Yolo Wonder plants was also assessed by quantitative DAS-ELISA.

PVY VPg and Pepper eIF4E Cloning

PVY SON41p[WT] and Yolo Wonder and HD285 eIF4E coding-sequences were introduced into Gateway pDONR-201 entry vector by performing attB-PCR with High-fidelity Phusion polymerase (NEB) and BP recombination reaction according to manufacturer's recommendations. Corresponding gene sequences and attB-primers are respectively listed in supplementary file S1 and table S3, Supplementary Material online.

PVY VPg Site-Directed Mutagenesis

Nucleotide substitutions corresponding to ID1, ID2, and OD2 VPg variants ($A_{280}G/T_{285}G/T_{300}A$, $A_{280}G/T_{285}A$, $G_{304}C/G_{340}C$, respectively) were introduced into the VPg-coding sequence of SON41p[WT] with the help of primers containing mutations (listed in supplementary table S3, Supplementary Material online), using Q5 site-directed mutagenesis kit (NEB). Mutated plasmids were recovered from bacterial clones using Wizard Plus SV Miniprep DNA Purification System kit (Promega) according to the manufacturer's instructions.

PVY VPg and Pepper eIF4E Production

Heterologous expression in *E. coli* was used to produce VPg and eIF4E proteins. VPg and eIF4E coding-sequences were cloned downstream from a hexa-histidine tag into bacterial expression plasmids pDEST17 Gateway vector (Invitrogen) and pETGB1a, respectively, following LR recombination and restriction/ligation standard procedures. Resulting vectors were used to transform expression bacterial strain BL21-AI (Invitrogen). Bacteria were grown at 37 °C until a DO_{600nm} value of 0.5. For protein expression induction, 0.1 M arabinose (pDEST17) and 0.2 M IPTG (pETGB1a) were added during 3 h at 28 °C. Bacterial culture lysates were prepared according to Michon et al. (2006). Total proteins were recovered in a Phosphate/NaF (pH 8) extraction buffer to prevent any far-UV background signal during CD measurements. Proteins of interest were purified by metal ion affinity chromatography, using Ni-NTA columns (Protino). Protein purity was checked by SDS-PAGE on 12.5% bis-acrylamide gels, followed by Coomasie blue total protein revelation and western blot using mouse antipolyHistidine antibodies (Sigma).

PVY Genomic RNA Isolation and Sequencing

Total RNAs were isolated from homogenates of upper symptomatic leaves using TRI-reagent kit (Sigma) and reverse-transcribed into cDNA using ReverTAID reverse-transcriptase (Thermoscientific). Full-length cDNA encoding PVY genomes and VPg cistrons were further PCR-amplified using primers flanking either the whole PVY genome or VPg cistrons. PCR products were sent to GENEWIZ Company or Genoscreen (Lille, France) for Sanger sequencing. All primer sequences are listed in supplementary table S3, Supplementary Material online.

Shannon Diversity Analysis

To compare the diversity of *pvr2³*-resistance-breaking variants between SON41p[ID2] and SON41[WT], Shannon diversity and corresponding 95% confidence intervals were calculated using an optimal nonempirical method described in Chao et al. (2013) using the Species-richness Prediction And Diversity Estimation in R [SpadeR]) online tool (Chao et al. 2016).

Determination of VPg/eIF4E In Vitro Interaction Affinity by Fluorescence Assays

All steady-state fluorescence acquisitions were obtained at 25 °C in 20 mM HEPES pH 7.5, 0.25 mM NaCl and 1 mM DTT using a SAFAS Xenius spectrofluorimeter (Monaco) equipped with a Peltier temperature controller. For optical characteristics of the instrument, see Michon et al. (2006). Affinity constants ($1/K_D$) were deduced from steady-state eIF4E tryptophan intrinsic fluorescence decrease upon titration by VPg as previously described in Michon et al. (2006). Measurements were performed by titration of a 0.25×10^{-6} M eIF4E solution. The VPg-eIF4E complex formation was titrated by 18–20 successive 2 µl additions of a 5×10^{-6} M VPg solution. After each VPg addition, eIF4E fluorescence emission was recorded for 2 min at 340 nm (excitation, 280 nm). The affinity constants of each of the VPg forms with eIF4E from Yolo Wonder and HD 285 were assessed by performing three simultaneous technical repetitions. Each of them included an interaction test with a m7-GTP cap analog as a positive control for eIF4E integrity and activity. Signal treatments and K_D determinations were performed by nonlinear regression following the method described in Michon et al. (2006). All measurements were performed twice using two different protein preparations for each of VPg and eIF4E.

Supplementary Material

Supplementary data are available at *Molecular Biology and Evolution* online.

References

Abdul-Razzak A, Guiraud T, Peypelut M, Walter J, Houvenaghel MC, Candresse T, Le Gall O, German-Retana S. 2009. Involvement of the cylindrical inclusion (CI) protein in the overcoming of an eIF4E-mediated resistance against Lettuce mosaic potyvirus. *Mol Plant Pathol.* 10(1):109–113.

Alves C, Cunha C. 2012. Order and disorder in viral proteins: new insights into an old paradigm. *Future Virol.* 7(12):1183–1191.

Ayme V, Petit-Pierre J, Souche S, Palloix A, Moury B. 2007. Molecular dissection of the potato virus Y VPg virulence factor reveals complex adaptations to the pvr2 resistance allelic series in pepper. *J Gen Virol.* 88(5):1594–1601.

Ayme V, Souche S, Caranta C, Jacquemond M, Chadœuf J, Palloix A, Moury B. 2006. Different mutations in the genome-linked protein VPg of potato virus Y confer virulence on the pvr2(3) resistance in pepper. *Mol Plant Microbe Interact.* 19(5):557–563.

Brown CJ, Johnson AK, Dunker AK, Daughdrill GW. 2011. Evolution and disorder. *Curr Opin Struct Biol.* 21(3):441–446.

Brown CJ, Johnson AK, Daughdrill GW. 2010. Comparing models of evolution for ordered and disordered proteins. *Mol Biol Evol.* 27(3):609–621.

Brown CJ, Takayama S, Campen AM, Vise P, Marshall TW, Oldfield CJ, Williams CJ, Dunker AK. 2002. Evolutionary rate heterogeneity in proteins with long disordered regions. *J Mol Evol.* 55(1):104–110.

Caranta C, Lefebvre V, Palloix A, Maraîchères P, Maurice S. 1997. Polygenic resistance of pepper to potyviruses consists of a combination of isolate-specific and broad-spectrum quantitative trait loci. *Mol Plant Microbe Interact.* 10:872–878.

Chao A, Wang YT, Jost L, Warton D. 2013. Entropy and the species accumulation curve: a novel entropy estimator via discovery rates of new species. *Methods Ecol Evol.* 4:1091–1100.

Chao A, Ma KH, Hsieh TC, Chiu CH. 2016. SpadeR (species-richness prediction and diversity estimation in R): an R package in CRAN.

Charon J, Theil S, Nicaise V, Michon T. 2016. Molecular BioSystems Protein intrinsic disorder within the Potyvirus genus: from proteome-wide analysis to functional. *Mol Biosyst.* 12:634–652.

Charron C, Nicolaï M, Gallois J-L, Robaglia C, Moury B, Palloix A, Caranta C. 2008. Natural variation and functional analyses provide evidence for co-evolution between plant eIF4E and potyviral VPg. *Plant J.* 54(1):56–68.

Chen JW, Romero P, Uversky VN, Keith A. 2006. Conservation of intrinsic disorder in protein domains and families: II. Functions of conserved disorder. *J Proteome Res.* 5(4):888–898.

Chroboczek J, Hébrard E, Mäkinen K, Michon T, Rantalainen K. 2012. Intrinsic disorder in genome-linked viral proteins VPgs of Potyviruses. In: Flexible viruses. Chichester, UK: John Wiley & Sons, Inc.

Cumberworth A, Lamour G, Babu MM, Gsponer J. 2013. Promiscuity as a functional trait: intrinsically disordered regions as central players of interactomes. *Biochem J.* 454:361–369.

Davenport MP, Loh L, Petravic J, Kent SJ. 2008. Rates of HIV immune escape and reversion: implications for vaccination. *Trends Microbiol.* 16(12):561–566.

Domingo E, Sheldon J, Perales C. 2012. Viral quasispecies evolution. *Microbiol Mol Biol Rev.* 76(2):159–216.

Drake JW. 1999. The distribution of rates of spontaneous mutation over Viruses, Prokaryotes and Eukaryotes. *Ann N Y Acad Sci.* 870(1 MOLECULAR STR):100–107.

Duffy S, Shackelton LA, Holmes EC. 2008. Rates of evolutionary change in viruses: patterns and determinants. *Nat Rev Genet.* 9(4):267–276.

Elena SF, Rodrigo G. 2012. Towards an integrated molecular model of plant–virus interactions. *Curr Opin Virol.* 2(6):719–724.

Gitlin L, Hagai T, LaBarbera A, Solovey M, Andino R, Perez DR. 2014. Rapid evolution of virus sequences in intrinsically disordered protein regions. *PLoS Pathog.* 10(12):e1004529

Grzela R, Szolajska E, Ebel C, Madern D, Favier A, Wojtal I, Zagorski W, Chroboczek J. 2008. Virulence factor of potato virus Y, genome-attached terminal protein VPg, is a highly disordered protein. *J Biol Chem.* 283(1):213–221.

Harrison BD. 2002. Virus variation in relation to resistance-breaking in plants. *Euphytica* 124:181–192.

Haynes C, Oldfield CJ, Ji F, Klitgord N, Cusick ME, Radivojac P, Uversky VN, Vidal M, Iakoucheva LM. 2006. Intrinsic disorder is a common feature of hub proteins from four eukaryotic interactomes. *PLoS Comput Biol.* 2(8):e100.

Hébrard E, Bessin Y, Michon T, Longhi S, Uversky VN, Delalande F, Van Dorsselaer A, Romero P, Walter J, Declerck N, et al. 2009. Intrinsic disorder in Viral Proteins Genome-Linked: experimental and predictive analyses. *Virol J.* 6:23.

Hulo C, Castro ED, Masson P, Bougueleret L, Bairoch A, Xenarios I, Mercier PL. 2011. ViralZone: a knowledge resource to understand virus diversity. *Nucleic Acids Res.* 39(Suppl 1):576–582.

Janzac B, Fabre F, Palloix A, Moury B. 2009. Constraints on evolution of virus avirulence factors predict the durability of corresponding plant resistances. *Mol Plant Pathol.* 10(5):599–610.

Jenner CE, Wang X, Ponz F, Walsh JA. 2002. A fitness cost for Turnip mosaic virus to overcome host resistance. *Virus Res.* 86(1–2):1–6.

Jiang J, Laliberté J-F. 2011. The genome-linked protein VPg of plant viruses – a protein with many partners. *Curr Opin Virol.* 1(5):347–354.

van der Lee R, Buljan M, Lang B, Weatheritt RJ, Daughdrill GW, Dunker AK, Fuxreiter M, Gough J, Gsponer J, Jones DT, et al. 2014. Classification of intrinsically disordered regions and proteins. *Chem Rev.* 114(13):6589–6631.

Martínez F, Rodrigo G, Aragonés V, Ruiz M, Lodewijk I, Fernández U, Elena SF, Daròs J-A. 2016. Interaction network of tobacco etch potyvirus NIa protein with the host proteome during infection. *BMC Genomics.* 17:87.

Michon T, Estevez Y, Walter J, German-Retana S, Le Gall O. 2006. The potyviral virus genome-linked protein VPg forms a ternary complex with the eukaryotic initiation factors eIF4E and eIF4G and reduces eIF4E affinity for a mRNA cap analogue. *FEBS J.* 273(6):1312–1322.

Montarry J, Doumayrou J, Simon V, Moury B. 2011. Genetic background matters: a plant–virus gene-for-gene interaction is strongly influenced by genetic contexts. *Mol Plant Pathol.* 12(9):911–920.

Moury B, Janzac B, Ruellan Y, Simon V, Ben Khalifa M, Fakhfakh H, Fabre F, Palloix A. 2014. Interaction patterns between potato virus Y and eIF4E-mediated recessive resistance in the Solanaceae. *J Virol.* 88(17):9799–9807.

Moury B, Morel C, Johansen E, Guilbaud L, Souche S, Ayme V, Caranta C, Palloix A, Jacquemond M. 2004. Mutations in potato virus Y genome-linked protein determine virulence toward recessive resistances in *Capsicum annuum* and *Lycopersicon hirsutum*. *Mol Plant Microbe Interact.* 17(3):322–329.

Nilsson J, Grahn M, Wright APH. 2011. Proteome-wide evidence for enhanced positive Darwinian selection within intrinsically disordered regions in proteins. *Genome Biol.* 12(7):R65.

Peng Z, Yan J, Fan X, Mizianty MJ, Xue B, Wang K, Hu G, Uversky VN, Kurgan L. 2014. Exceptionally abundant exceptions: comprehensive characterization of intrinsic disorder in all domains of life. *Cell Mol Life Sci.* 72(1):137–151.

Pepin KM, Lass S, Pulliam JRC, Read AF, Lloyd-Smith JO. 2010. Identifying genetic markers of adaptation for surveillance of viral host jumps. *Nat Rev Microbiol.* 8(11):802–813.

Pfeiffer JK, Kirkegaard K. 2005. Increased fidelity reduces poliovirus fitness and virulence under selective pressure in mice. *PLoS Pathog.* 1(2):0102–0110.

Rantalainen KI, Uversky VN, Permi P, Kalkkinen N, Dunker A. k, Makinen K. 2008. Potato virus A genome-linked protein VPg is an intrinsically

disordered molten globule-like protein with a hydrophobic core. *Virology* 377(2):280–288.

Roudet-Tavert G, Michon T, Walter J, Delaunay T, Redondo E, Le Gall O. 2007. Central domain of a potyvirus VPg is involved in the interaction with the host translation initiation factor eIF4E and the viral protein HcPro. *J Gen Virol*. 88(Pt 3):1029–1033.

Sanjuán R, Nebot MR, Chirico N, Mansky LM, Belshaw R. 2010. Viral mutation rates. *J Virol*. 84(19):9733–9748.

Scholthof K-BG, Adkins S, Czosnek H, Palukaitis P, Jacquot E, Hohn T, Hohn B, Saunders K, Candresse T, Ahlquist P, et al. 2011. Top 10 plant viruses in molecular plant pathology. *Mol Plant Pathol*. 12(9):938–954.

Sickmeier M, Hamilton JA, LeGall T, Vacic V, Cortese MS, Tantos A, Szabo B, Tompa P, Chen J, Uversky VN, et al. 2007. DisProt: the database of disordered proteins. *Nucleic Acids Res*. 35(Database issue):D786–D793.

Tokuriki N, Oldfield CJ, Uversky VN, Berezovsky IN, Tawfik DS. 2009. Do viral proteins possess unique biophysical features? *Trends Biochem. Sci*. 34(2):53–59.

Uversky VN. 2002. Natively unfolded proteins: a point where biology waits for physics. *Protein Sci*. 12:2–12.

Wang A, Krishnaswamy S. 2012. Eukaryotic translation initiation factor 4E-mediated recessive resistance to plant viruses and its utility in crop improvement. 13:795–803.

Woody RW. 2010. Circular dichroism of intrinsically disordered proteins. In: Uversky VN, Longhi S, editors. Instrumental analysis of intrinsically disorered proteins: assessing structure and conformation. p. 303–321.

Wright PE, Dyson HJ. 1999. Intrinsically unstructured proteins: reassessing the protein structure–function paradigm. *J Mol Biol*. 293(2):321–331.

Xue B, Blocquel D, Habchi J, Uversky AV, Kurgan L, Uversky VN, Longhi S. 2014. Structural disorder in viral proteins. *Chem Rev*. 114(13):6880–6911.

Xue B, Dunbrack R, Williams R, Dunker AK, Uversky VN. 2010. PONDR-FIT: a meta-predictor of intrinsically disordered amino acids. *Biochim Biophys Acta*. 1804(4):996–1010.

Xue B, Dunker AK, Uversky VN. 2012. Orderly order in protein intrinsic disorder distribution: disorder in 3500 proteomes from viruses and the three domains of life. *J Biomol Struct Dyn*. 30(2):137–149.

Xue B, Mizianty MJ, Kurgan L, Uversky VN. 2012. Protein intrinsic disorder as a flexible armor and a weapon of HIV-1. *Cell Mol Life Sci*. 69(8):1211–1259.